Methodology in Hydrology (Proceedings of the Second International Symposium on Methodology in Hydrology held in Nanjing China October–November 2005) IAHS Publ 311 2007

Large flood prediction in poorly gauged basins: the 2004 largest-ever flood in Fukui, Japan

YASUTO TACHIKAWA[1], RYOICHI TAKUBO[1], TAKAHIRO SAYAMA[2] & KAORU TAKARA[2]

1 *Department of Urban and Environmental Engineering Kyoto University Kyoto 615-8540 Japan*
tachikawa@mbox kudpc.kyoto-u ac jp

2 *Disaster Prevention Research Institute Kyoto University Kyoto 611-0011 Japan*

Abstract In the Asuwa River basin in Fukui Prefecture Japan, the largest-ever flood since hydrological observations began, occurred on 18 July 2004. The severe rainfall front in the middle of July brought a heavy rainfall of 265 mm in six hours. The urban area of Fukui was heavily inundated due to dyke breaks along the Asuwa River; the upper parts of the Asuwa River basin were also severely damaged by flood and sediment disasters. When establishing flood control planning in Japan, obtaining a design flood estimated by using a rainfall–runoff model with a design rainfall having some exceedence probability is fundamental. However, the accumulation of hydrological data for estimating design floods is insufficient, especially in small-scale basins. In particular, information about large floods near or above the magnitude of a design flood is less available. In this study, we examine how well/bad the largest-ever 2004 flood in Fukui, Japan is predicted using a state of the art physically-based distributed rainfall–runoff model; then we discuss sources of flood prediction uncertainty and an approach for reducing the uncertainty and enhancing the reliability of flood discharge prediction.

Keywords prediction in ungauged basins; flood control planning; runoff model; PUB

INTRODUCTION

In 2004, severe rainfall fronts and ten typhoons hit Japan and caused heavy rainfall disasters with 232 casualties. These disasters mainly occurred in tributary catchments of several hundreds of square kilometres in size. River management of these catchments are organized by prefectural governments; in most situations, the river improvements still do not reach a designed safety level. It is not easy to achieve the high river improvements in the future.

For these catchments, assessing the safety level of the current state of the river basins is the basis for designing a future river development programme. Also, to develop a real-time flood runoff prediction system to issue flood warnings is a crucial measure to save lives. To achieve these purposes, hydrological predictions by a reliable rainfall–runoff model are fundamental.

On the other hand, the accumulations of hydrological data are usually insufficient for this purpose, especially for small-scale catchments of several hundred square kilometres. The floods in small scale basins are generally sensitive to spatial and temporal distributions of rainfall patterns. Therefore flood runoff predictions for small-scale basins require more detailed hydrological information than for large-scale basins with more than several thousand square kilometres. In addition, the flood data with a magnitude of a design flood level, or above that level, does not exist in most situations. In this sense, rainfall–runoff models are not validated for estimating a flood with the magnitude of a design level. Thus testing a rainfall–runoff model for predicting a historical largest-ever flood under the limitations of the available hydrological data and analysis of the cause of the difference between predicted and observed floods is a basis for improving the prediction and so to reduce flood disasters.

The peak discharge of the 2004 Fukui flood is estimated as about 2400 m^3/s by MLIT, the Ministry of Land, Infrastructure and Transport in Japan. This peak discharge is more than two times larger than any other recorded floods since discharge observation began in 1978, and was caused by the concentrated heavy rainfall. The catchment mean values of maximum rainfall in six hours, and in two days, are 265 and 297 mm; the return periods of which are estimated as about 1000 and 25 years, respectively, by MLIT.

In this paper, we apply a physically-based distributed rainfall–runoff model based on topographic representations using grid-based DEMs and kinematic flow routing (Shiiba *et al*, 1999; Ichikawa *et al*, 2001; Tachikawa *et al*, 2004) to the upper part of the Asuwa River basin (351 km^2); then examine the predictability of the distributed runoff model for the 2004 Fukui flood; and finally discuss the source of flood prediction uncertainty and a direction to reduce the uncertainty and enhance the reliability of flood discharge prediction.

DISTRIBUTED RAINFALL-RUNOFF MODEL

Topographic representation using DEMs

Figure 1 illustrates the catchment topographic model using DEMs processed with the algorithms by Shiiba *et al* (1999). A slope segment is represented by a rectangle formed by the adjacent two grid points determined to have the steepest gradient. In Fig. 1, three flow lines connect to grid point A and two flow lines to grid point B; thus 1/3 of grid area A and 1/2 of grid area B are given to form the area of the slope segment AB. The slope width is determined by dividing the area by the slope length AB. The catchment topography is represented as a set of slope segments. Figure 2 shows the topography model of the Asuwa River basin (351 km^2) and Fig. 3 is an enlarged illustration of the upper part of the study area. The spatial resolution of DEMs used here is 50 m.

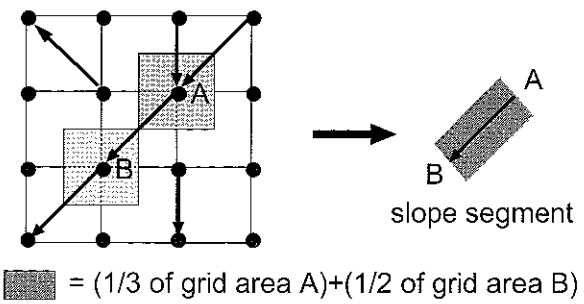

Fig. 1 Catchment topography modelling by Shiiba *et al* (1999).

Flow routing model

According to the flow directions shown in Fig. 2, the slope flow is routed one-dimensionally. The slope discharge is given to the river flow routing model; then the river flow is routed to the outlet. In each slope segment, the slope is assumed to be covered by a permeable soil layer composed of a capillary soil layer and a non-capillary soil layer. In the soil layers, slow flow and quick flow are modelled as unsaturated Darcy flow with variable hydraulic conductivity and saturated Darcy flow with constant hydraulic conductivity. If the depth of water exceeds the soil water capacity, overland flow happens. These processes are represented with a kinematic wave model using a function for the discharge–stage relationship (Tachikawa *et al*, 2004):

$$q=\begin{cases} v_m d_m (h/d_m)^{\beta}, & 0 \le h < d_m \\ v_m d_m + v_a (h-d_m), & d_m \le h < d_a \\ v_m d_m + v_a (h-d_m) + \alpha (h-d_a)^m, & d_a \le h \end{cases} \quad (1)$$

as illustrated in Fig. 4 and the continuity equation:

$$\frac{\partial q}{\partial x}+\frac{\partial h}{\partial h}=r \quad (2)$$

where q is discharge with unit width; h is flow depth; r is rainfall intensity; $v_m = k_m i$, $v_a = k_a i$, $k_m = k_a/\beta$, $\alpha = \sqrt{i}/n$; i is gradient of the slope segment; k_m is saturated hydraulic conductivity of the

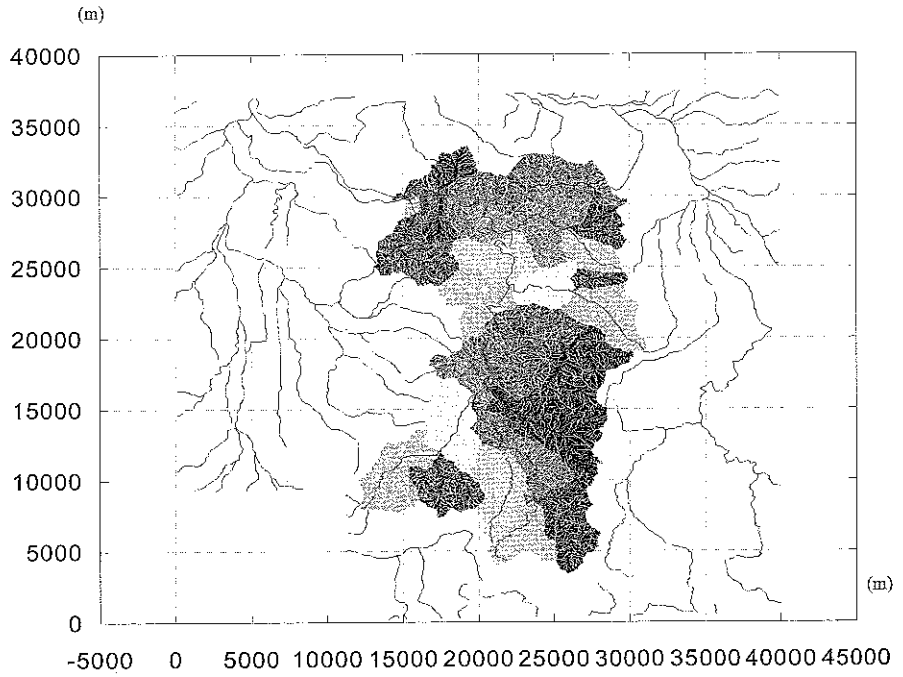

Fig. 2 Watershed model for the Asuwa River basin with the upper part of the Tenjinbashi station. The location is specified using UTM coordinates with m unit.

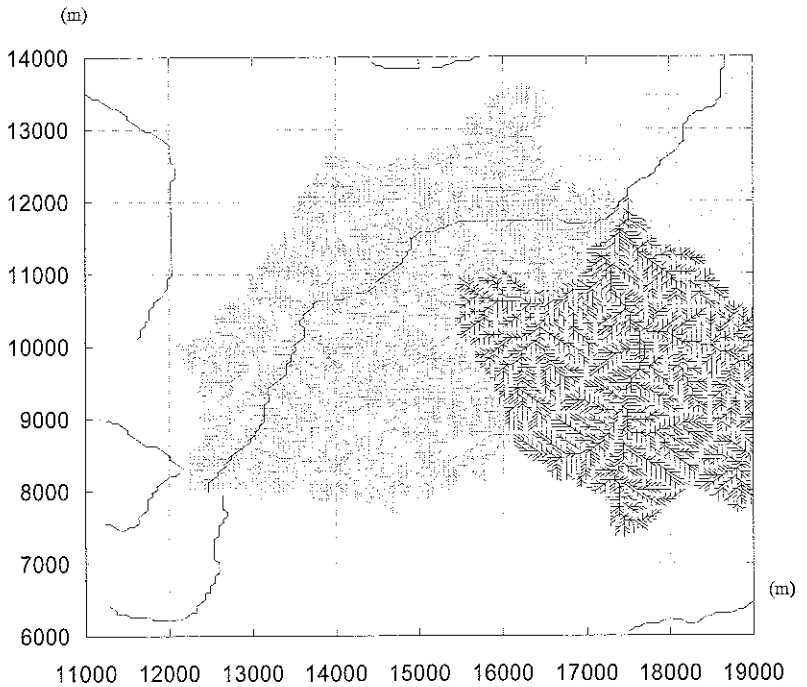

Fig. 3 Enlarged illustration for the uppermost stream of the Asuwa watershed model.

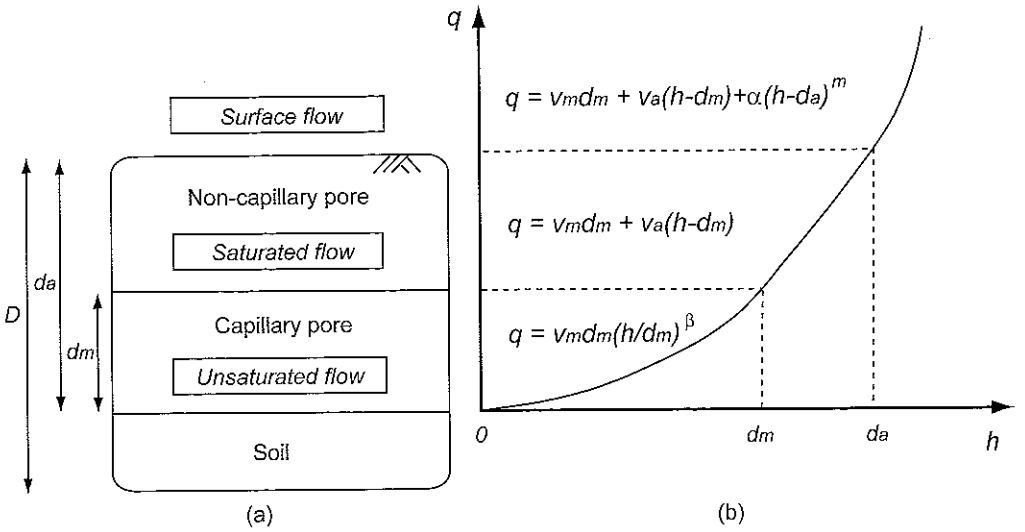

Fig 4 (a) Model soil structure, and (b) discharge stage relationship

capillary soil layer; k_a is hydraulic conductivity of the non-capillary soil layer; n is surface roughness coefficient; d_m is the capacity water depth for the capillary soil layer; and d_a is the capacity water depth including capillary and non-capillary soil layers. The model parameters to be determined are n ($m^{-1/3}s$), k_a (m/s), d_a (m), d_m (m), and β. For river flow routing, surface flow with a rectangular cross section is assumed for the kinematic wave approximation.

PARAMETER ESTIMATION AND FLOOD SIMULATIONS

Nine floods with peak discharges of more than 400 m^3/s were selected from the discharge data since 1978. For each flood, spatial distributions of hourly rainfall with 3-km grid resolution were generated from the ground-gauged rainfall measurements using the nearest neighbour method; then the five model parameters described above that define the function of the stage–discharge relationship in equation (1) were determined. At first, the model parameter values identified at other catchments are set; next the values of water storage capacity d_a and d_m are calibrated to fit the observed and simulated hydrographs by the trial-and-error method. Then the values of k_a and β are optimized, if needed. The initial water depth at each slope segment is determined from the initial river discharge at the outlet using the kinematic wave model, assuming the steady state condition. Therefore, each runoff simulation starts at a time long enough after the previous flood event and before the intended flood begins. For river routing, the Manning roughness coefficient is set to 0.03 $m^{-1/3}s$ for all cross sections.

Table 1 summarizes the results of parameter identifications. To evaluate the appropriateness of the simulated discharges, the peak discharge ratio P_r and the Nash-Sutcliffe efficiency N_s:

$$P_r = Q_{s\ peak} / Q_{o\ peak} \tag{3}$$

$$N_s = 1 - \Sigma(Q_o - Q_s)^2 / \Sigma(Q_o - \overline{Q}_o)^2 \tag{4}$$

are used, where Q_o and Q_s represent observed and simulated discharge at one hour interval; $\overline{Q}_o$ is the time average of Q_o in simulation duration. Tables 2 and 3 summarize the results of the goodness of fit. In these tables, each row represents the evaluation value for each flood using the model parameter values identified for the intended year. In Table 2, the P_r values between 0.85 and 1.15 are not shaded while those less than 0.85 or greater than 1.15 are shaded. In Table 3, the N_s values less than 0.70 are shaded.

Table 1 Model parameter values fitted to each year flood and the characteristics of each year heavy rainfall and flood discharge

Properties	Group 1 (overestimating peak discharge)			Group 2 (over/under-estimating peak discharge)			Group 3 (underestimating peak discharge)		
Parameters	1993	1981	1982	1985	1983	1979	1989	1990	2004
n ($m^{-1/3}s$)	0 4	0 4	0 4	0 4	0 4	0 4	0 4	0 4	0 4
k_a (m/s)	0 01	0 03	0 01	0 01	0 03	0 01	0 01	0 01	0 01
d_a (m)	0.25	0 4	0 2	0 2	0 6	0 17	0.25	0 325	0 26
d_m (m)	0 18	0 35	0 15	0 1	0 15	0 1	0 18	0 2	0 16
d_o-d_m (m)	0 07	0 05	0 05	0 1	0 45	0 07	0 07	0 125	0 10
β (-)	24	24	12	8	12	4	4	8	4
Peak discharge (m^3/s)	548	1117	676	542	758	622	608	447	2400
Initial discharge (m^3/s)	11	65	18	86	36	37	44	17	25
6 hour rainfall R_{6h} (mm)	60	73	42	43	54	84	67	56	265
2 days rainfall R_{2d} (mm)	116	163	136	116	169	103	174	127	297
Rainfall ratio R_{6h}/R_{2d}	0.52	0 45	0 31	0.37	0.32	0 82	0.39	0.44	0.89
Station number	10	4	7	10	4	6	10	10	12

Table 2 Evaluation of goodness of fit using peak discharge ratio. In the column for 1993, the peak discharge ratio of each year flood predicted using the parameter values identified with the 1993 flood are shown.

Flood	Peak discharge ratio using the parameter identified for each year									Mean
	1993	1981	1982	1985	1983	1979	1989	1990	2004	
1993	1 03	0 86	0 91	0.77	0.49	0.69	0.42	0.47	0.47	0 68
1981	0 87	0 88	0 90	0.74	0.60	0.72	0.45	0.48	0.45	0 68
1982	1.02	0 92	0 94	0 87	0.49	0 87	0.46	0.48	0.45	0 72
1985	1 13	0 96	1 06	1.00	0 89	0 91	0.62	0.73	0.62	0 88
1983	1.08	1 03	1 08	0.99	0 91	0 91	0.68	0.75	0.71	0 90
1979	1.77	1.61	1.65	1.17	0 96	1 02	0.52	0.64	0.48	1 09
1989	1.23	1.33	1.20	1.20	1.08	1.13	0 94	0 95	0 91	1 11
1990	1.84	1.65	1.75	1.60	1.42	1.44	0 90	1 04	0 97	1 40
2004	1.85	1.71	1.82	1.58	1.26	1.55	1 08	1.12	1.00	1.44
Mean	1 31	1.22	1.26	1.10	0 90	1 03	0.67	0.74	0.67	0.99

Table 3 Evaluation of goodness of fit using the Nash-Sutcliffe model efficiency measures. In the column for 1993, the Nash-Sutcliffe measures of each year flood predicted using the parameter values identified with the 1993 flood are shown.

Flood	Nash-Sutcliffe model efficiency measures using the parameter identified at each year									Mean
	1993	1981	1982	1985	1983	1979	1989	1990	2004	
1993	0 97	0 93	0 95	0 92	0.62	0 88	0.61	0.67	0.61	0 79
1981	0.95	0 95	0 95	0 92	0.82	0 92	0.66	0 71	0.68	0 84
1982	0.67	0 86	0 92	0 80	0 86	0 80	0.69	0 71	0.64	0 77
1985	0 91	0 87	0 84	0 94	0 91	0 97	0 79	0 90	0 79	0 88
1983	0.94	0.95	0.95	0 98	0.95	0 97	0 84	0 90	0 86	0 93
1979	0.22	0.52	0.51	0 73	0.50	0 78	0 74	0 74	0 70	0 61
1989	0.66	0.78	0.72	0.82	0.88	0.90	0 88	0 93	0 79	0 82
1990	0.16	0.48	0.38	0.45	0.11	0.61	0 76	0.74	0 76	0 49
2004	0.12	0.25	0.00	0.49	0.12	0.60	0 95	0.95	0.95	0.47
Mean	0.62	0.73	0.69	0 78	0.61	0.82	0.77	0.81	0.75	0.73

The results suggest that the identified model parameter sets can be classified into three groups: Group 1 with the 1993, 1981 and 1982 floods; Group 2 with the 1985, 1983 and 1979 floods; and Group 3 with the 1989, 1990 and 2004 floods. The parameter sets in Group 1 have a tendency to overestimate and those in Group 3, to underestimate floods; and Group 2 shows both tendencies. Figure 5 shows the simulated hydrographs of the 2004 flood using the parameter sets identified for each flood. The estimated peak discharges are widely distributed between 2500

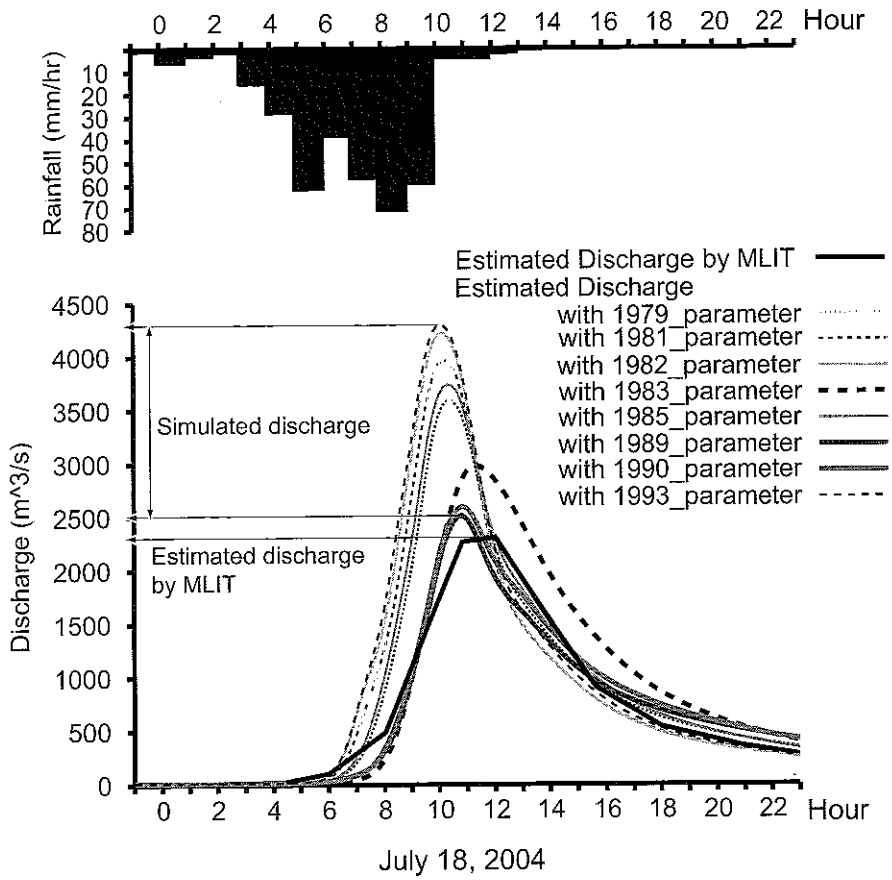

Fig 5 Reproduction of 2004 flood with identified parameter values

and 4200 m^3/s, and are larger than the estimated peak discharge 2400 m^3/s obtained by MLIT from hydraulic river flow simulations with the high flood stage marks.

DISCUSSION

Within each group, the values of model parameters are close, and the floods simulated with any parameter set show good scores of the peak ratio and the Nash efficiency. The clear difference among the groups is that in Group 1 the value of β is larger and the capacity of the non-capillary layer $d_a - d_m$ is smaller as compared to Group 3. The difference in parameter values comes from the different hydrological characteristics. In Group 1, rainfall stored in the soil layer flows quite slowly. In this case, river discharge is insensitive to rainfall intensity at the beginning of a flood, and the soil layer is easily saturated. Once the water depth on slope segments exceeds the capacity of the capillary soil water, river discharge suddenly increases. The thin non-capillary layer readily generating surface flow supports the effect. In contrast, the parameter sets in Group 3 tend to show the opposite characteristics so that the discharge hydrograph increases from the beginning of rainfall and its peak discharge is smaller than when the same rainfall is given to the runoff model with parameter sets in Group 1. Group 2 shows features between those of the groups 1 and 3.

The question is why the difference is observed in the same catchment. Each group includes various scales of floods and there are no distinguishing characteristics in the rainfall and discharge

data to form the three groups. One clear difference is the number of rainfall gauging stations. All floods in Group 3 were observed with more than 10 rainfall stations. It is inferred that the accuracy of the rainfall observations affects the value of the calibrated model parameters and the wrong parameter values cause large prediction uncertainty.

Another possible reason for the large prediction uncertainty is the setting of the initial condition for prediction simulations. Groups 1 and 2 include a flood observed with 10 rainfall stations. The difference among the floods with more than 10 rainfall stations is the amount of the observed/estimated initial discharge. The 1993 flood has the smallest initial discharge; while the 1985 flood has the largest initial discharge in these floods. For the 1985 flood, the recession of river discharge is clearly observed. This implies that it was not correct for the 1985 flood to assume the steady state condition at the beginning of simulation. Rainfall is spatially distributed and the distributions are memorized in the spatial distribution of soil moisture, thus if the initial condition setting is inappropriate the resultant model parameter values are wrongly obtained.

For the 1993 flood, a sudden increase of river discharge followed dry conditions. To simulate the flood with the distributed rainfall–runoff model used here, it is necessary to set β to a large value to retain water in the soil layer for continuing small discharge. If the low flow observation in 1993 is correct, the improvement of model structure, including the refinement of the discharge–stage relationship and the initial condition setting are the key to improve the flood runoff prediction by the runoff model used here.

CONCLUSIONS

A physically based rainfall–runoff model used here showed large uncertainty in predicting the largest ever flood in Fukui that occurred in 2004. In this research, the cause of prediction uncertainty was discussed. It was inferred that the uncertainty comes from the insufficiency of the hydrological data, the inadequate setting of the initial condition, and the inadequacy of the hydrological model structure. To predict floods for small-scale catchments, more detailed hydrological information is required. To improve the prediction accuracy, more hydrological data observations are vital. Unfortunately it is not easy to set and maintain observation systems. In this situation, the direction to make better prediction is to express the prediction uncertainty with an appropriate measure and clarify the cause of the uncertainty quantitatively. When we have a measure of prediction uncertainty, the improvement of a hydrological model can be evaluated in terms of how the model decreases prediction uncertainty. Furthermore, we could know the priority of the activities we should take to improve the prediction accuracy.

REFERENCES

Ichikawa, Y., Murakami, M., Tachikawa, Y. & Shiiba, M. (2001) Development of a basin runoff simulation system based on a new digital topographic model. *J. Hydraulic, Coastal and Environ. Engng JSCE* **691**(II-57), 43–52.

Shiiba, M., Ichikawa, Y., Sakakibara, I. & Tachikawa, Y. (1999) A new numerical representation form of basin topography. *J. Hydraulic, Coastal & Environ. Engng JSCE* **621**(II-47), 1–9.

Tachikawa, Y., Nagatani, G. & Takara, K. (2004) Development of stage–discharge relationship equation incorporating saturated-unsaturated flow mechanism. *Ann. J. Hydraulic Engng JSCE* **48**, 7–12.